Cyclic delamination failure in CFRP-strengthened reinforced concrete beams

G P A G van Zijl[1], A J Badenhorst[2]

[1] Civil Engineering Department, Stellenbosch University, South Africa, gvanzijl@sun.ac.za
[2] Element Consulting Engineers, Namibia

This is an original scientific paper published in Concrete Beton, journal of the Concrete Society of Southern Africa, in Volume 148, pp 18-25, March 2017.

Journal Contact Details:
PO Box 75364
Lynnwood Ridge
Pretoria, 0040
South Africa
+27 12 348 5305

admin@concretesociety.co.za
www.concretesociety.co.za

Cyclic delamination failure in CFRP-strengthened reinforced concrete beams

G.P.A.G. van Zijl[1] and A.J. Badenhorst[2]

[1]Civil Engineering Department, Stellenbosch University, South Africa, gvanzijl@sun.ac.za

[2]Currently, Element Consulting Engineers, Namibia

ABSTRACT

Strengthening of reinforced concrete (RC) beams with Carbon Fibre Reinforced Polymer (CFRP) strips is widely done to successfully restore or increase RC capacity. Delamination of externally bonded CFRP strips from concrete is an important failure mode. Bond-slip relations have been proposed by several authors for quasi-static, monotonic delamination, but not yet for delamination during load cycles as experienced for instance by bridge beams subjected to vehicle loads. In this contribution, cyclic delamination of CFRP strips from RC beams is investigated. A simple, small-scale physical test is developed to study quasi-static and cyclic delamination in the vicinity of a flexural crack in the RC substrate. The results are used to calibrate a finite element (FE) model, which is subsequently used to analyse the cyclic delamination under a range of cyclic load levels. The computed responses confirm the role of a flexural crack in the RC in initiating delamination. Also, initiation of delamination can be distinguished in cases of lower cyclic load levels, before abrupt pull-off of the CFRP strips. The number of load cycles to compete pull-off reduces significantly with increased cyclic load level.

INTRODUCTION

Methods of strengthening infrastructural elements are in demand to ensure or extend their service life, or to increase their load bearing capacity beyond that originally designed for in cases of upgraded functionality. Here, the focus is on the strengthening of existing bridge beams by means of Carbon Fibre Reinforced Polymer (CFRP) strips bonded onto the tensile face of the reinforced concrete (RC) beams. Of particular interest is the delamination of the CFRP strip from the beam face in the vicinity of a flexural crack in the concrete.

In addition to the failure modes of concrete crushing and steel bar yield or rupture, the structural designer must consider CFRP rupture, as well as delamination of the CFRP strip from the concrete substrate. Delamination initiation and propagation depend on the mechanical properties of the substrate concrete, the adhesive material used to attach the CFRP strip, and on the properties of the interface between the substrate and repair system. The delamination failure may occur along the actual substrate-CFRP strip interface, or, in case of relatively weak substrate concrete, within the concrete (Buyukozturk et al. 2003). In the latter case, delamination may occur close to the substrate surface, or at the level of the steel bar reinforcement, whereby the cover concrete is delaminated from the steel reinforcing bars (Smith and Teng 2011). Delamination typically occurs in regions of high stress, or at a discontinuity, such as a flexural or shear crack in the concrete (Teng et al. 2002; Smith and Teng 2002).

In previous studies on fatigue, improvement of fatigue behaviour by CFRP strengthening was reported and ascribed to lowered stresses in steel reinforcement by crack width limitation of CFRP-reinforcement (El-Tawil et al. 2001). Failure of CFRP-strengthened RC beams under fatigue loading has been found to be due to rupture of steel reinforcement (El-Tawil et al. 2001; Al-Hammoud et al. 2011). Barnes and Mays (1999) have presented fatigue results in term of applied stress range *(S)* versus the number of cycles *(N)* to failure. These so-called *S-N* curves were determined from cyclic tests on only three RC beams strengthened with CFRP strips, and each tested at a different stress range, for up to more than 10 million load cycles. The fatigue failure involved steel bar rupture. *S-N* curves were also reported by Al-Hammoud et al. (2011) for CFRP strip-strengthened RC beams, in which rebar rupture was the final fatigue failure mode. Cyclic delamination of the CFRP strips from the RC beam may however, be the dominant fatigue failure mode, as demonstrated by Badenhorst (2012). Aidoo et al. (2002) also observed delamination of CFRP strips in their fatigue tests on FRP-strengthened RC beams, which led to load transfer to the steel reinforcing bars and eventual rupturing of these steel bars. Bond-slip relations have been proposed by Lu et al. (2004) and Smith and Gravina (2005) for quasi-static, monotonic loading conditions, which assist in determining the load at onset of delamination, as well as the rate of delamination. However, to the authors' knowledge, measured data or bond-slip models for cyclic delamination have not yet been reported in the literature.

This paper reports a combined physical and computational experimental program towards characterising such cyclic delamination. The CFRP strip reinforcement pull-off bond-slip behaviour is tested under monotonic loading conditions to capture the full bond-slip relation. Subsequently, cyclic pull-off tests are performed at various loading cycle ranges to observe the cyclic delamination and number of cycles to failure. The interfacial shearing resistance is characterised by separate mechanical tests, and subsequently used in nonlinear finite element modelling with the DIANA (2009) package to simulate the cyclic delamination, and to extrapolate the physical test results to more loading ranges.

EXPERIMENTAL PROGRAM

A combined physical experimental and computational research program was designed to study cyclic delamination of CFRP strips from RC elements. The following sections describe the physical laboratory experiments. The study was limited to a single concrete class of 35 MPa cube strength, produced with a single binder type (CEM I 42,5), RC concrete specimens containing a single crack with a surface width of 0.2 mm, and a single CFRP strip type.

Test specimens

The RC T-section specimen shown in Figure 1 was designed for the purpose of the CFRP strip pull-off tests. It features a 250 mm long web with a 150 mm x 150 mm cross-section. The specimens were reinforced with 2 Y10 steel bars, i.e. two bars of nominal diameter 10 mm and characteristic yield stress of at least 450 MPa. A minimum cover depth of 20 mm to the CFRP-bonded concrete face was maintained. The specimens were cast in specially designed moulds. From the same mix batch, 100 mm cubes were cast for testing the compressive strength. The specimens were stripped after 1 day and cured in water at 23 ± 2°C for another 6 days, after which they

were removed from the curing tanks and kept in laboratory conditions until the age of 21 days.

The specimens were then pre-cracked in a Zwick Z250 MTM as illustrated in Figure 1b. This was done by bolting down the specimen to the test bed, and gripping the two protruding 10 mm steel bars at the top in the MTM upper clamp. To ensure the crack location at a height of 100 mm from the specimen top, notches of 20 mm deep and 5 mm wide were sawn. The crack width was carefully controlled by two linear variable differential transformers (LVDTs) to a surface width of 0.2 mm.

After the pre-cracking, the protruding steel bars were ground off at the top surface of the specimen. A CFRP strip was subsequently applied to the face of the web where the crack formed. A 50 mm wide by 1.4 mm thick CFRP strip (Mapei 2016) was applied to the front face over a nominal length of 250 mm, but extended upward beyond the specimen's upper face for the purpose of gripping in the upper clamp of the Zwick Z250, as shown in Figure 1c. An epoxy layer of roughly 1 mm thick was applied. The specimens were then left until the age of 35 days to allow the epoxy to harden in the laboratory environment.

Concrete and epoxy property characterisation

The concrete compressive strength was determined by cube crushing tests in a Contest 1 MN MTM. Three cubes were cast, cured and tested from the same batch of concrete prepared for each specimen type, as summarised in Table 1.

The shear strength of the epoxy-bonded connection was tested in separate tests on specimens prepared from the same concrete mix and curing regime. So-called triplet test specimens were prepared, containing a central concrete plate of 42 mm thick, and 150 mm x 150 mm height and depth. The concrete plate was bonded on each face to a 25 mm thick steel plate, as shown in Figure 2a. The same epoxy was used as for the CFRP strip attachment in the T-section pull-off tests, and the joints were also roughly 1 mm thick.

The triplet test setup is shown in Figure 2a. The upper bearing plate forced the central concrete plate to shear off at the epoxy joints with the steel plates, which were supported by steel rollers. Note that the use of steel plates for the shear bond tests was justified by delamination occurring in the concrete in all cases, as can be seen clearly in Figure 2b, but also in the CFRP pull-off tests. Note that shear failure was forced to occur in the left hand side joint (Figure 2a), by applying the epoxy over the central 110 mm x 110 mm of the steel plate and concrete interface only. This can be seen clearly in Figure 2c.

Three specimens were tested, controlled by the displacement measured by the LVDT shown in Figure 2a. The three measured

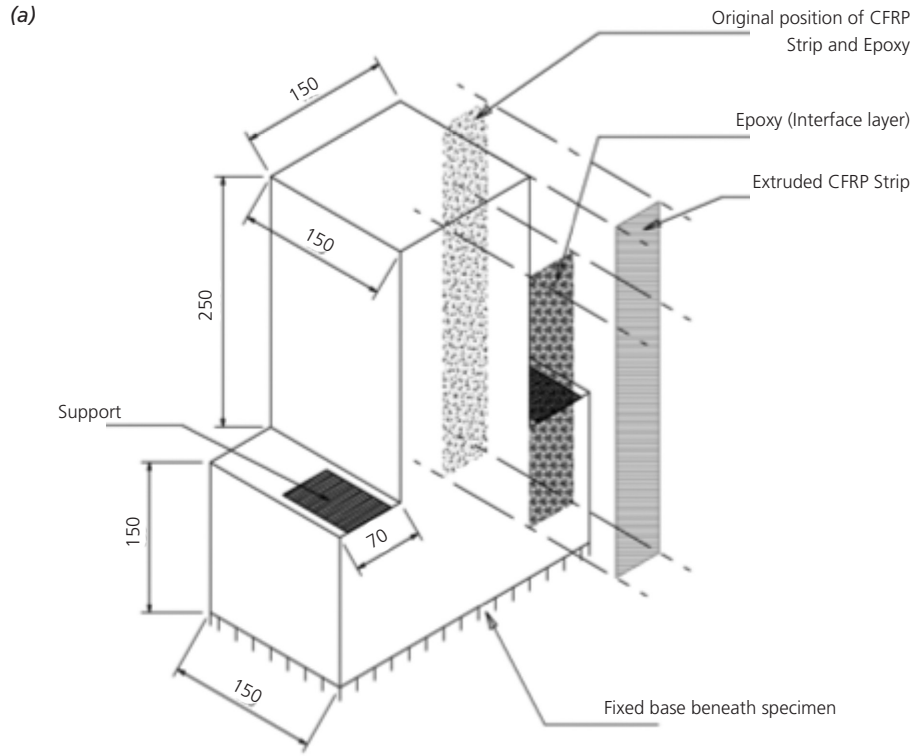

Figure 1. T-section specimen (a) geometry (dimensions in mm), (b) bolted test setup for pre-cracking, (c) bolted test setup for CFRP pull-off test, showing the (d) pull-off displacement measurement relative to the top face

Table 1. Concrete cube compressive strength

Test	Specimen	Compressive strength (MPa)	
		Average	Standard deviation
Triplet	All	44.3	1.1
Pull-off tests for bond strength	T-section 1	40.2	1.3
	T-section 2	43.4	0.9
	T-section 3	44.5	1.3
	T-section 4	46.4	1.0

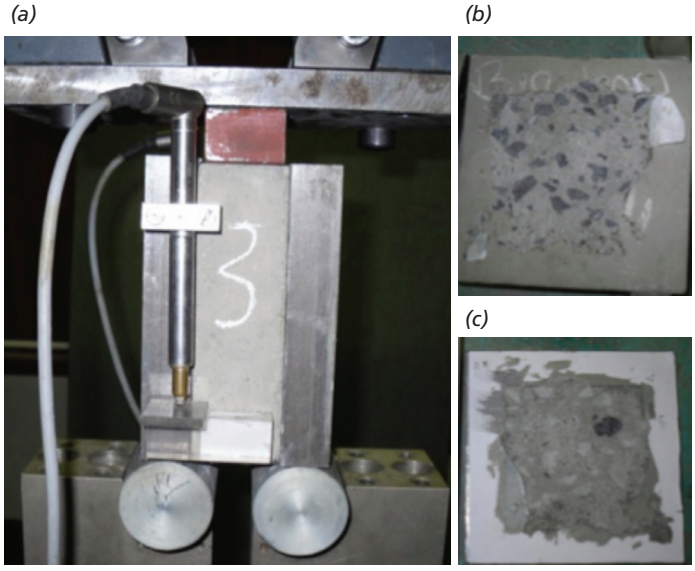

Figure 2. Triplet test (a) setup in Zwick MTM, showing the (b) debonded concrete face and (c) steel plate after the test

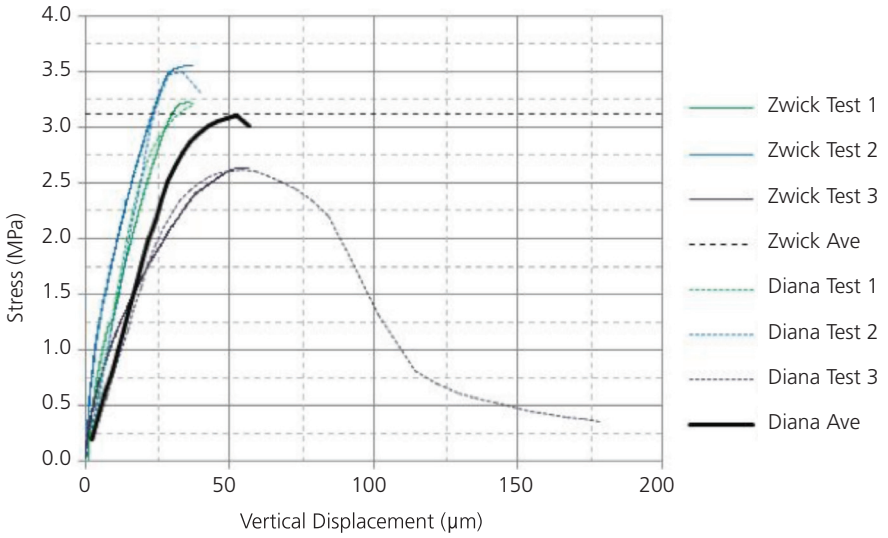

Figure 3. Triplet experimental shear stress-displacement responses

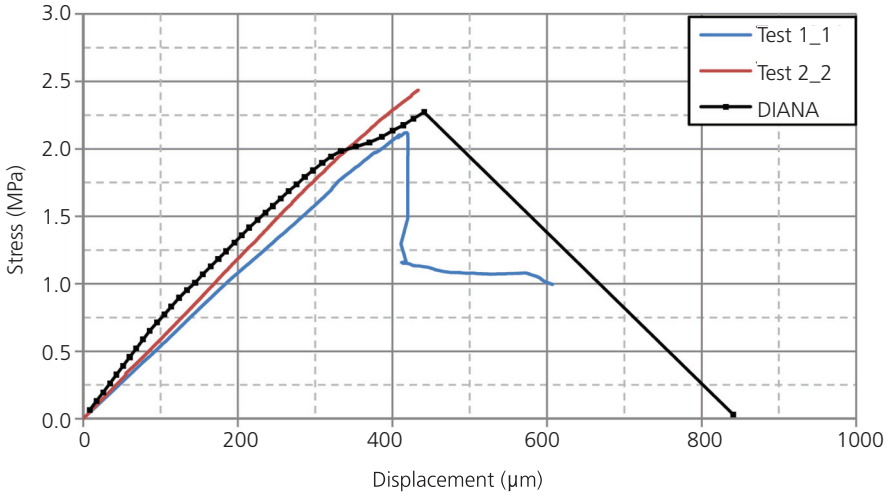

Figure 4. T-section CFRP-strip pull-off response

average stress-displacement responses are shown in Figure 3. An average epoxy bond shear strength of about 3.1 MPa was determined in this way.

Experimental pull-off tests

Monotonic pull-off test

The four T-section specimens were tested in the configuration shown in Figure 1c, d. Two specimens (T-sections 1 and 2 in Table 1) were tested by displacing the lower bed of the Zwick Z250 MTM downward at the constant rate of 0.05 mm per minute. The relative displacement of the CFRP strip and the T-section upper face was captured (Figure 1d), enabling the shear stress-deformational response to be captured as shown in Figure 4. Note that the pull-off force was divided by the bonded area of the CFRP strip, resulting in the averaged pull-off stress represented on the vertical axis of Figure 4. The linear ascending stress-deformation branches were followed by abrupt pull-off of the CFRP strips. This is reflected by the sudden vertical drop in average shear stress in Test 1 (T-section 1) shown in Figure 4, followed by a post-peak horizontal stress-displacement response. However, for T section 2, which had an about 14% higher maximum bonded shear strength than T section 1, no post-peak response could be measured, due to the abrupt, unstable delamination following the peak.

It should also be noted that the peak values of about 2.1 and 2.4 MPa are significantly less than the average shear strength of 3.1 MPa obtained from the triplet tests. This is explained by the variability in the shear strength, seen in the triplet test results of Figure 3. Another reason lies in the averaging of the pull-off

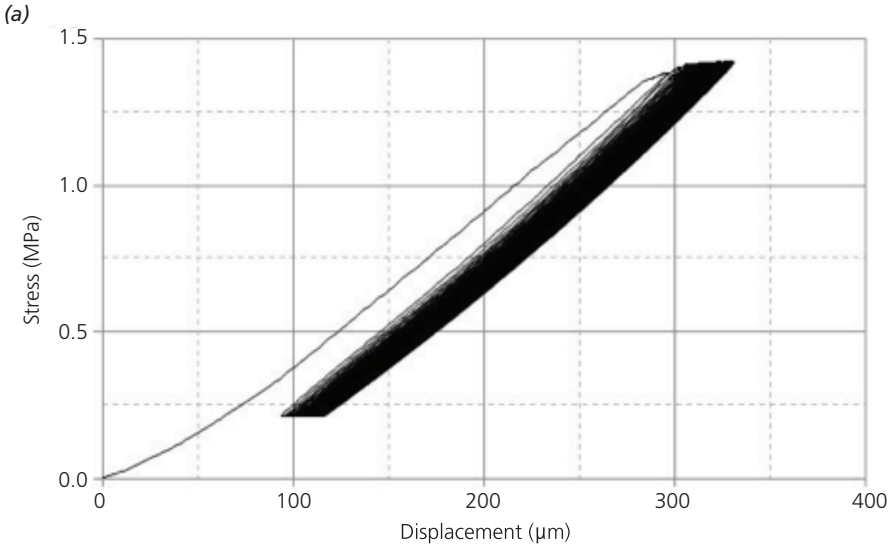

Figure 5. (a) Experimental response to cyclic response of T-section 4 to 65%, and (b) a failed specimen loaded cyclically to 85% of the static pull-off resistance

stress by division with the full bonded area of 50 mm x 250 mm. While this is roughly the same bonded area size as in the triplet test (110 mm x 110 mm), the elongated CFRP bond is postulated to cause a more significantly non-uniform shear stress distribution over the 250 mm length.

Cyclic pull-off test

Subsequently, T-section specimens 3 and 4 (Table 1) were tested under cyclic loading to 85% and 65% respectively of the peak static pull-off resistance. In Figure 5a the cyclic response is shown for the 65% case. The load was cycled between the former respective upper bounds and a lower value of 10% of the static resistance, accounting to some extent for permanent load. The cyclic loading was applied under displacement control, at the same displacement rate of 0.05 mm per minute as for the monotonic test. For all T-section tests the final failure was by full delamination as shown by the photo insert in Figure 5b. The number of cycles to failure was 26 at 85% and 300 at 65% of the average peak load.

COMPUTATIONAL MODELLING

To extend the experimental range, computational modelling was used to firstly capture the experimentally observed response, and subsequently analyse more cases.

FE model

The T-section test was modelled in a finite element (FE) approach. The FE model is shown schematically in Figure 6. Linearly interpolated, plane stress membrane elements of dimension 5 mm x 5 mm were used to model the concrete. Plane stress interface elements, each with a length of 5 mm to match the quadrilateral elements of the concrete section, were placed horizontally in the position of the pre-crack, in order to simulate the tension-free response across the pre-cracked region. Similar interface elements were used to model the epoxy bond between the concrete and CFRP plate. Embedded steel reinforcing bars were modelled in the position of the steel reinforcing bars' centroid axis. The CFRP plate was modelled with beam elements, matching the 5 mm long interface elements and 5 mm high quadrilateral (concrete) elements described above. The bolted connection to hold the T-section in position during the pull-off test (Figure 1c) was also modelled with beam elements, connected to the concrete T-section and fixed at the lower end at the MTM test bed.

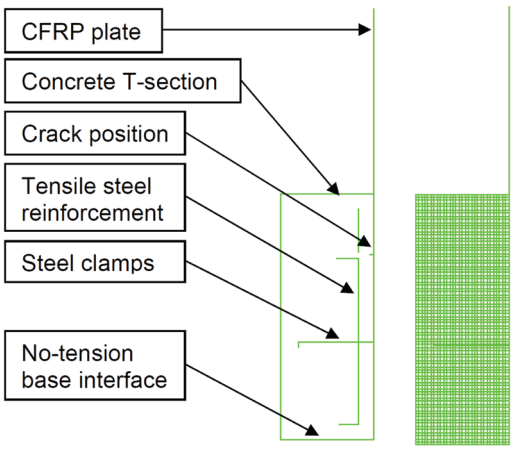

Figure 6. 2D plane stress FE model of the T-section test

Material models

Linear elastic behaviour was modelled for the concrete and the CFRP strip, whereby inelasticity was restricted to the concrete pre-crack (no-tension) and the epoxy joint. For the concrete a Young's modulus of E_c = 35 GPa and Poisson's ratio of v = 0.2 were prescribed, and for the CFRP E_{CFRP} = 200 GPa. For the steel reinforcing bar the elastic parameters were E_s = 210 GPa and v = 0.2, while a Von Mises perfect plasticity model was used, with a yield stress of 550 MPa. However, the steel bars remained elastic in all cases.

The epoxy interface model is based on multi-surface plasticity, combining a Coulomb-friction limit function with a tension cut-off and a compression cap, as depicted in Figure 7. As crushing was not expected or observed in the T-section tests, the compressive cap was deactivated. Both the Coulomb-friction and tension cut-off modes allow fracture energy-based softening, as depicted by the shrinking

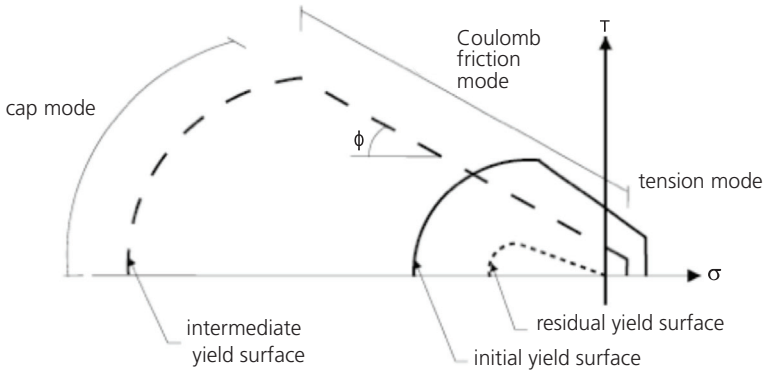

Figure 7. Interface model used for the no-tension pre-crack, as well as the epoxy bond

failure surfaces drawn by dashed and dotted lines in Figure 7. The shearing adhesion of the epoxy bond, which in fact included shearing within the concrete as shown in the photo inserts in Figures 2 and 5, were calibrated to the triplet test results, leading to a virgin shearing adhesive strength of c = 3.1 N/mm^2 and shearing fracture energy G_F^{II}= 0.35 N/mm. The initial tensile strength was set to f_t = 3.1 N/mm^2 and tensile fracture energy G_F^I = 0.045 N/mm. The epoxy interface stiffness was assigned as k_n =110 N/mm^3 and k_s = 65 N/mm^3 in the normal and shearing direction respectively, to match the overall elastic deformation. Note that these model parameter values led to reasonable agreement shown in Figure 3 between the (average) FE analysis response and the average measured response of the triplet tests. For detailed description of the calibration process, the reader is referred to Badenhorst (2012). There, plane stress FE modelling and analysis of the three characterisation triplet tests are described, of which the computational responses are also shown in Figure 3.

The pre-crack was modelled by considering complete separation at the crack location to a depth of 50 mm into the concrete. The interface elements representing the remaining 100 mm of the potential crack were assigned reasonable tensile properties for concrete of this class, namely f_t = 3.5 N/mm^2 and tensile fracture energy G_F^I = 0.05 N/mm.

FE RESULTS OF T-SECTION MODELS

Static FE tests

The computed response for the monotonic test, simulated by deformation control of the CFRP upper end, is compared with the two measured responses for T-sections 1 and 2 in Figure 4. The computed initial stiffness is slightly higher than the measured stiffness, but the peak resistance and deformation are captured with reasonable accuracy.

Note that the computed post-peak response was unstable, possibly indicating snap-back. This confirms the abrupt nature of the post-peak responses observed in the physical experiments. No attempt was made to use arc length methods to computationally follow the snap-back response suggested by the T-section 1 response. Thus, the straight post-peak line represents a single numerical step beyond the peak, skipping over the expected brittle post-peak response. An attempt to capture this brittle response should incorporate numerical crack mouth opening displacement control along the interface representing the epoxy bond. This was considered not to be essential for the subsequent analyses of the current research.

Cyclic FE tests

The 85% (T-section 3) and 65% (T-section 4) cyclic tests were simulated computationally by using time steps and prescribed cyclic force evolutions. The computed responses are shown in Figure 8 together with the computed monotonic response.

The experimental failure was more sudden than in the computed response, which included a number of load cycles with significantly increased permanent deformation shortly before failure in the computed responses. In the physical experiments, such larger load cycle responses could not be observed or captured. Nevertheless, the computed and observed numbers of cycles to failure are in reasonable agreement, as shown in Table 2. Exactly the same number of load cycles (26) to failure was found for the computed and physically tested case at 85%. However, the computed response to the 65% case indicates 300 cycles to failure, while CFRP pull-off was observed after 196 cycles in the physical experiment. The CFRP pull-off displacement is shown as function of the number of loading cycles for these two cases in Figure 9, as further illustration of the computational and experimental responses for T-sections 3 and 4.

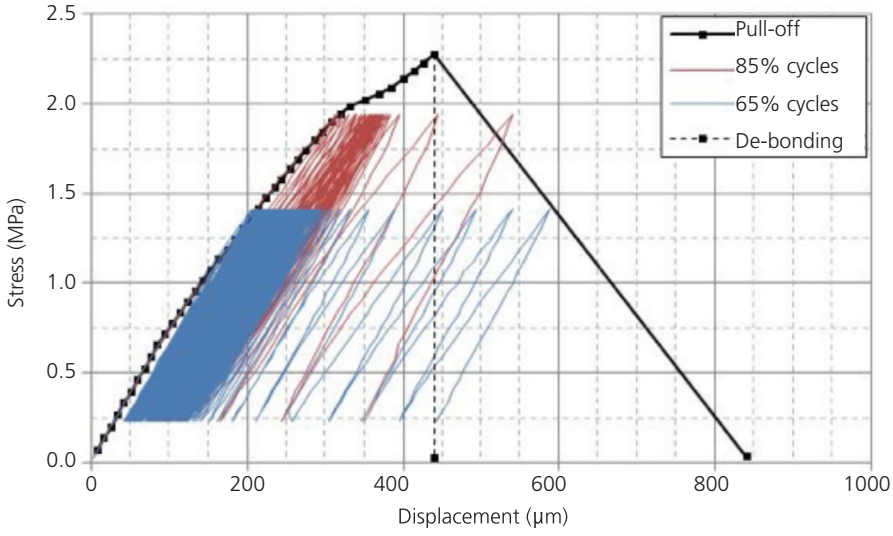

Figure 8. Computed cyclic responses

Table 2. Number of cycles to delamination thresholds

Cyclic load level	Damage initiation	Unstable pull-off	
	DIANA	DIANA	Experimental
85%	-	26	26
75%	-	78	-
65%	4	196	300
55%	15	280	-
45%	40	1000	-

The CFRP pull-off displacement is shown as function of the number of loading cycles for these two cases in Figure 9, as further illustration of the computational and experimental responses for T-sections 3 and 4. The evolution of computed and observed deformation with load cycles is not identical, with a more sudden final pull-off observed in the experiment than computationally. Nevertheless, the overall deformation and number of cycles are considered to be captured to a reasonable level of accuracy. Based on this reasonable agreement, the model was used to analyse responses to other levels of cyclic loading, namely 75%, 55% and 45% of peak static pull-off resistance. The expected trend of an increased number of loading cycles to complete pull-off was found. Table 2 summarises the computed numbers of cycles to failure and Figure 10 shows the number of cycles to initiation and final pull-off of the CFRP strip graphically.

DISCUSSION OF MEASURED AND COMPUTED RESPONSES

As elaborated in the previous section, reasonable agreement was found between the computed and observed responses for the static pull-off tests (T-sections 1 and 2), as well as for the two cyclic tests (85% - T-section 3, 65%- T-section 4). Based on this agreement, more cases were analysed with the FE model, namely cyclic loadings to an upper load value of 75%, 55% and 45% of the average quasi-static peak load respectively. The number of computed cycles to failure for these cases is summarised in Table 2.

Shear-slip at the crack

The crack in the T-section specimen, caused in the initial, pre-cracking step illustrated in Figure 1b, simulates a flexural crack in a beam, on its tensile face where the CFRP strip is attached in CFRP strip strengthening of such a RC beam. The influence of this 0.2 mm wide crack on the CFRP strip delamination response is considered next.

Figure 11 shows the relations between shear-slip deformation in the interface element directly above the pre-crack in the T-section and the number of load cycles. Three stages of inelastic deformation can be observed, namely an initial zero or small gradient of "damage" evolution, followed by a secondary branch of higher damage rate, and finally the onset of quick, unstable CFRP pull-off.

A closer analysis of the inelastic shear-slip deformation in the CFRP-concrete bond directly above the concrete crack shows that

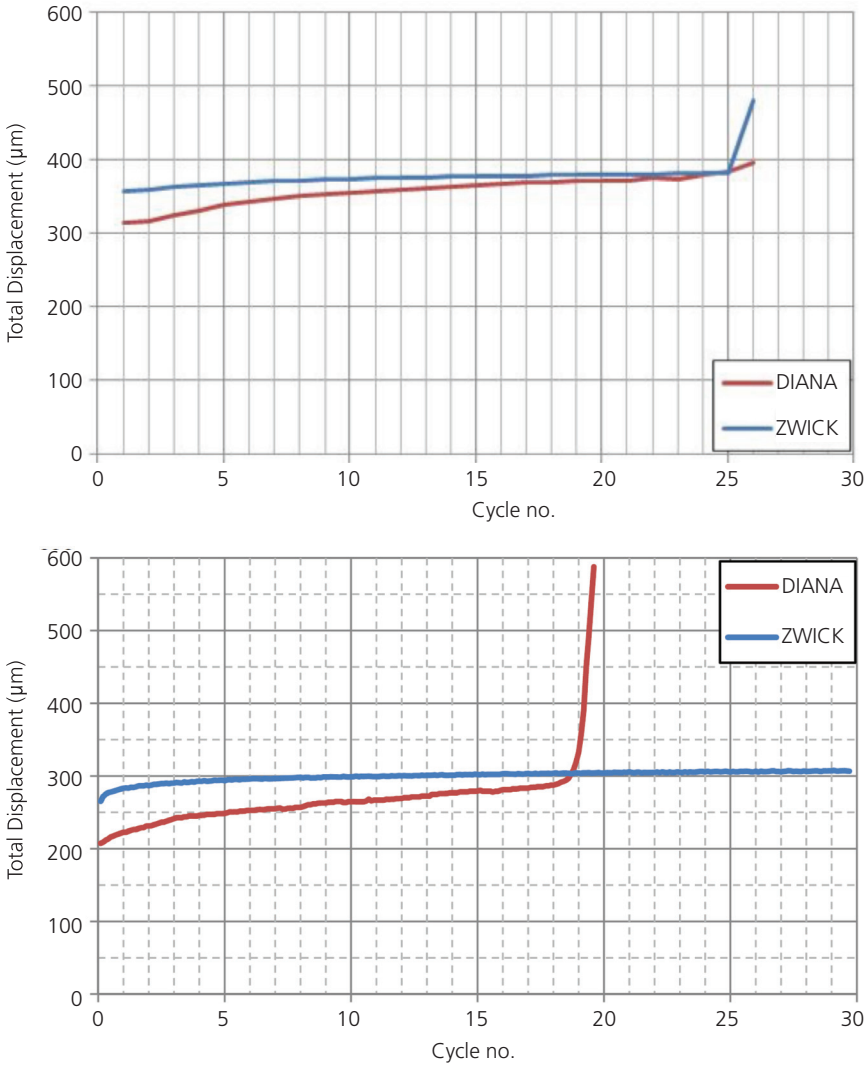

Figure 9. Total relative shearing displacement under cyclic load of (top) 85% and (bottom) 65% of static resistance

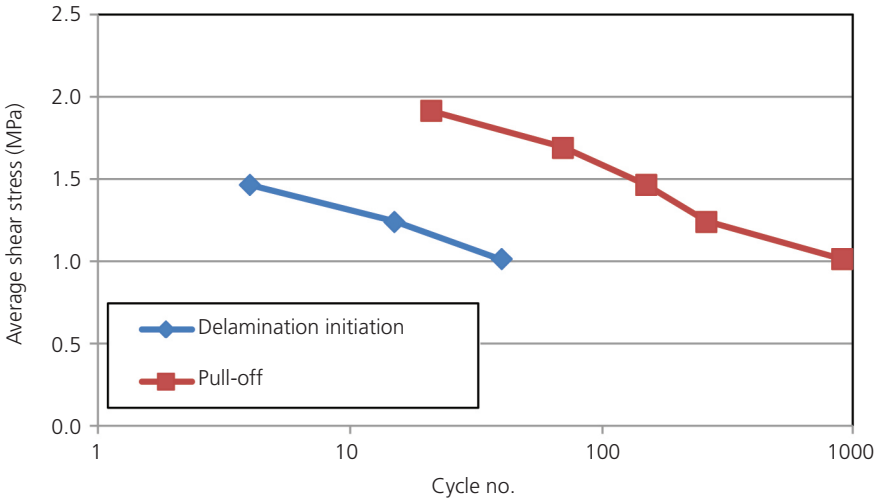

Figure 10. Computed number of cycles to shear-slip initiation and final pull-off

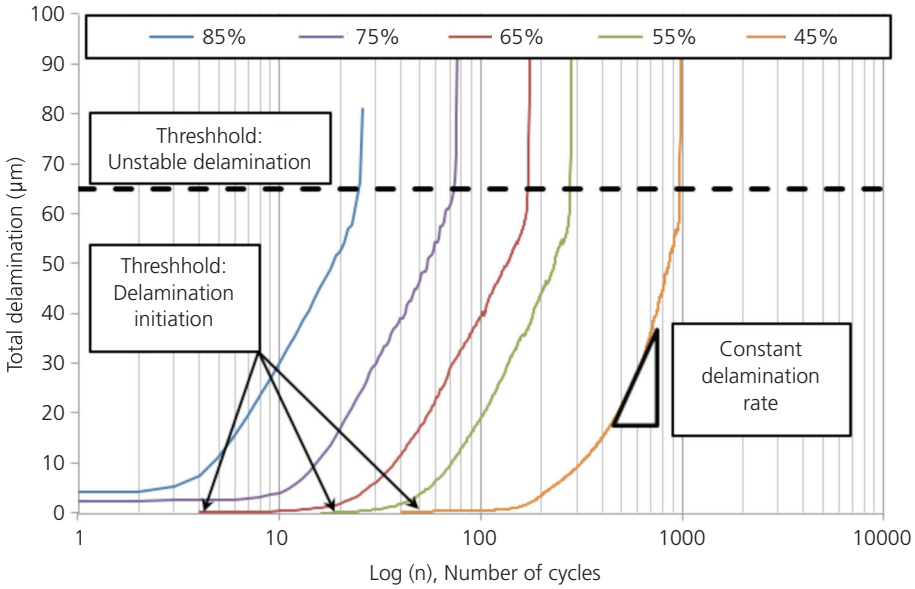

Figure 11. Inelastic shear-slip deformation in the interface directly next to a crack in the concrete

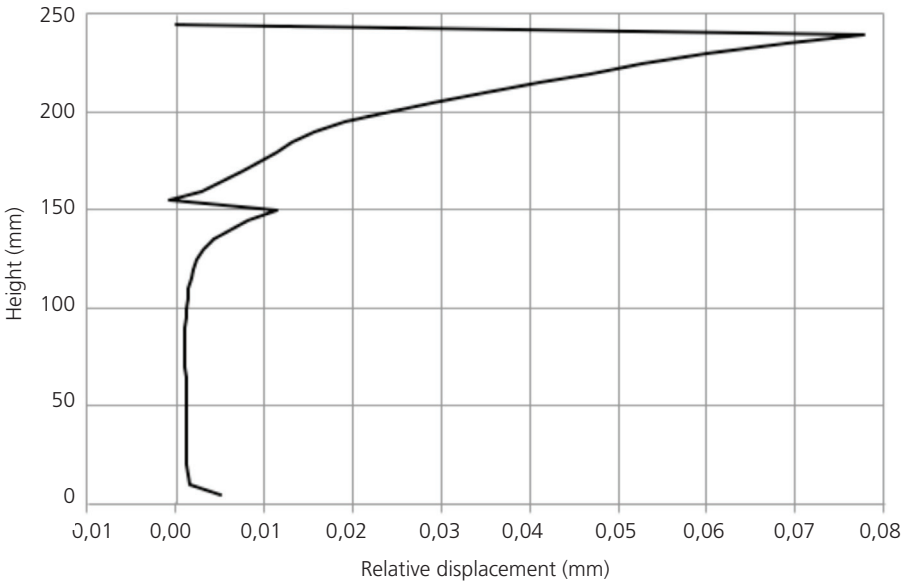

Figure 12. Computed shear-slip in the epoxy interface between the RC T-section and the CFRP strip

for large cyclic loads, in this case 75% and 85% of static resistance, the first load cycle leads to permanent, inelastic shear-slipping deformation. However, for smaller cyclic loads, a load-dependent threshold number of loading cycles exists before inelastic deformation is initiated in the bonded interface. The number of cycles to such damage initiation has also been listed in Table 2 and shown graphically in Figure 10.

A near constant threshold level of inelastic shear-slipping deformation before unstable delamination appears to exist. This is indicated with a dashed line in Figure 11. In all the analysed cases (45% - 85%) unstable pull-off follows once an inelastic shear-slip of roughly 60 to 65 µm is reached.

Accelerated cyclic pull-off

It must be born in mind that the T-section should be considered to be an accelerated bond fatigue test. An overall axial tension force acts in combination with a bending moment, and tensile normal separation occurs between the RC and CFRP at the upper face of the concrete in the T-section. This does not occur in the interface between a bonded CFRP strip on an actual RC beam loaded in flexure. The extent of shear-slip deformation along the height of the epoxy bond between the CFRP strip and the concrete T section is shown in Figure 12. From the graph it is clear that the situation close to final pull-off contributes to the CFRP pull-off. Note that the 0.2 mm wide concrete (pre-)crack is at the position 150 mm and the upper concrete face at position 250 mm in Figure 12. In follow-up research the influence of the upper discontinuity and mixed mode delamination will be studied in order to derive a link with the delamination process in the vicinity of a flexural crack or cracks in a RC beam.

ADRIAAN BADENHORST
(MScEng, PrEng) is a professional engineer at Element Consulting Engineers, Namibia and has over 5 years' experience in the civil engineering industry. His skills include drafting of structural plans, structural and civil design, construction supervision, project management, structural condition assessments and report writing as well as feasibility studies of potential projects. He has been involved in projects of residential, commercial, industrial and institutional nature.

GIDEON VAN ZIJL
(PhD, PrEng) is professor of Structural Engineering at Stellenbosch University since 2001. His research interests are structural and computational mechanics, structural durability and advanced cement-based construction materials. Concurrently, structural design guidelines for cement-based construction materials are developed in his research group, the Centre for Development of Sustainable Infrastructure (CDSI).

CONCLUSIONS

The shear-slip delamination process in epoxy bonded interfaces between RC beams and CFRP strip reinforcing has been studied in a combined physical and computational experimental program. A small scale T-section test has been proposed for monotonic as well as cyclic testing of the bond-slip behaviour. The test results were simulated with reasonable accuracy in FE computational modelling, which was subsequently used to analyse more cases of cyclic bond-slip behaviour. The following conclusions are drawn:

- Fatigue failure of CFRP strip strengthened RC beams may be caused by cyclic delamination of the CFRP strip from the concrete substrate. In the specimens tested here, the failure mechanism in all static and cyclic tests was full and abrupt delamination of the CFRP strip and the concrete substrate skin.
- A crack causes discontinuity in the concrete face, leading to the CFRP strip delamination.
- In the accelerated test reported here, a cyclic load as low as 45% of the peak static resistance leads to failure by CFRP strip pull-off. It remains to be established whether a lower threshold load level exists for which pull-off does not occur, irrespective of the number of loading cycles, i.e. whether a fatigue limit exists.
- Delamination initiates after a threshold number of loading cycles. This threshold depends on the load level. For high cyclic loads, here 75% and 85% of the peak static pull-off resistance, delamination initiates in the first cycle. For lower loads, a number of stress cycles (4 at 65%, to 40 at 45% of the peak static resistance) is required before delamination initiates.
- A constant threshold shear-slip displacement of the CFRP strip is reached at the position of a concrete flexural crack, before abrupt and complete pull-off follows. In the cases studied here, this threshold shear-slip was in the range of 60 to 65 μm. This is postulated to depend on the particular materials, and is likely to be governed by the elastic and fracture properties such as shear-slip fracture energy.
- The link of this accelerated fatigue test to fatigue of CFRP strengthened RC beams remains to be clearly established, to allow the design of such CFRP strengthening for particular loading cycle scenarios based on accelerated test data. ▲

REFERENCES

Aidoo, J., Harries, K.A., Petrou, M.F. (2002). *Fatigue behaviour of CFRP-Strengthened reinforced concrete bridge girders.* Columbia, SC: University of South Carolina.

Al-Hammoud, R., Soudki, K., Topper, T.H. (2011). Fatigue flexural behaviour of corroded reinforced concrete beams repaired with CFRP sheets. *ASCE Journal of Composites for Construction*, 15(1):42-51.

Badenhorst, A.J. (2012). *Debonding of External CFRP Plates from RC Structures Caused by Cyclic Loading Effects*. MScEng-thesis, Stellenbosch University, Stellenbosch.

Barnes, R.A., Mays, G.C. (1999). Fatigue performance of concrete beams strengthened with CFRP plates. *ASCE Journal of composites for construction*, 3(2):63-72.

Buyukozturk, O., Gunes, O., Karaca, E. (2003). Progress on understanding de-bonding problems in reinforced concrete and steel members strengthened using FRP composites. *Construction and Building Materials*, 18:9-19.

DIANA (2009). *Diana finite element analysis software version 9.3*, TNO Diana, The Netherlands.

El-Tawil, S., Ogunc, C., Okeil, A., Shahawy, M. (2001). Static and fatigue analyses of RC beams trengthened with CFRP laminates. *Journal of composites for construction*, 5(4): 258-266.

Lu, X.Z., Teng, J.G., Ye, L.P., Jiang, J.J. (2004). Bond-Slip models for FRP sheet/plate-to-concrete interfaces. In: Proceedings of the *2nd International Conference on advanced polymer composites for structural applications in construction (ACIC2004)*, Woodhead Publishing Limited, Cambridge, pp. 152-161.

Mapei South Africa (Pty) Ltd. (n.d.). Retrieved from http://www.mapei.co.za

Smith, S.T., Teng, J.G. (2002). FRP-Strengthened RCbeams. I: Review of de-bonding strength models. *Engineering Structures*, 24: 385-395.

Smith, S., Gravina, R., (2005). Critical de-bonding length in FRP flexurally strengthened RC members. In: Proceedings of the *International Symposium on Bond Behaviour of FRP in Structures (BBFS 2005)*, pp. 269-274.

Teng, J., Chen, J., Smith, S., Lam, L. (2002). *FRP Strengthened RC Structures*. Chichester, West Sussex, England: John Wiley & Sons, Ltd.